**Journal of Engineering and Development, Vol.19, No.2, march. 2015, ISSN 1813- 7822**

# *Behavior of Reinforced Modified Reactive Powder Concrete Knee Joints*

*Asst. Prof. Dr. Jasim Mahmud Al-Khafaji*
*Civil Eng. Dept.*
*Al- Mustansiriyah University*

*Lec.Dr. Haider Abdul Ameer*
*Civil Eng. Dept.*
*Al- Mustansiriyah University*

*Wael Shahatha*
*Environmental Eng. Dept.*
*Al-Mustansiriyah University*

## *Abstract*

***This investigation presents an experimental study of strength and behavior of Modified Reactive Powder Concrete (MRPC) corner subjected to bending moment tended to open the angle. Twelve specimens are tested to study the corner strength, cracks types, cracking moment, cracks patterns, corner deflection, ductility and corner efficiency. Ten MRPC knee joints were mixture of steel fiber, superplasticized, silica fume-cement blended with very low water/cement ratio (w/c) characterized by very fine sand (maximum size 600μm), where the presence of natural crushed aggregate of maximum size (4.75mm) was used to replace a part of the fine sand. The rest two corners of Normal Strength Concrete (NSC) which are the mixture of (1:1.5:3) (cement : sand 4.75mm : gravel 10mm). The specimens are designed to represent an actual prototype of a portal frame corner. The compressive strength of concrete in the test varies from (23.5) to (88.9) MPa, and steel tension ratio in legs is constant, ρ = 0.008, for ten specimens where the two MRPC corners are plain concrete. The specimens are designed to represent an actual prototype of a portal frame corner. The nominal dimensions of the tested corners are (1078 mm) in overall length, (600 mm) in height, the cross section of the corner is rectangular (212×150mm). All corners are supported to be hinged in one leg by two clamps and rolled in other leg, also all corners are loaded by steel frame where, it produces moment tends to open the angle. Concrete strains are recorded for each tested corner; also load deflection curves were plotted. Throughout the test operation crack***

*patterns were drawn and the mode of failure of the tested corners is identified, which is divided into two types (flexural and bearing) failure. It was found that enhance the properties of concrete for corner block improve efficiency to be such an alternative solution for corner block contain stirrups and complicated details of rebar. Depending on the results of the current experimental work a sufficient corner was recommended for building subjected to seismic and earthquake regions.*

**Keywords: NSC, MRPC, Corner, Steel fiber, Silica Fume, ratio of fine sand to fine gravel.**

# سلوك وصلات خرسانية مسلحة قائمة الزاوية من خرسانة المساحيق الفعالة المعدلة

ا.م.د. جاسم محمود الخفاجي
قسم الهندسة المدنية/الجامعة المستنصرية

د . حيدر عبد الأمير
قسم الهندسة المدنية/الجامعة المستنصرية

وائل شحاذة عبد الكريم
قسم هندسة البيئة/الجامعة المستنصرية

**الخلاصة:**

يستعرض البحث الحالي دراسة عملية لمقاومة وتصرف أنواع متعددة من تفاصيل التسليح للأركان الخرسانية المعرضة لعزوم إنحناء تعمل على فتح الزاوية .تم فحص (12) نموذج لدراسة تأثير مقاومة الخرسانة، نوع التشققات، عزوم التشققات، أشكال التشققات، المطيلية بالاضافة الى هطول الركن الخرساني وكفاءته .صممت النماذج لكي تمثل وتحاكي أركان الهياكل الإنشائية .مقاومة إنضغاط الخرسانة العادية (23.5 ميكا باسكل ) وللخرسانة الفعالة المعدلة تراوحت بين (55.3 و88.9) ميكا باسكل ،ونسبة حديد الشد في سيقان الأركان كانت ثابتة وتساوي 0.008 لعشرة نماذج مفحوصة تحتوي على حديد التسليح في حين كان نموذجين خاليين من حديد التسليح . صممت النماذج لكي تمثل وتحاكي أركان الهياكل الإنشائية ،أبعاد النماذج هي (1078 ملم) طولا و (600 ملم) للارتفاع و (150 ملم) سمكا . إما المقطع العرضي كان مربعا في الساق (150×150 ملم) ومستطيلا في القاعدة (150×212 ملم). أسندت جميع الأركان على شكل مفصلي في أحد السيقان بإستخدام عقفتين وأسندت الجهة الأخرى بمفصل متحرك . تم تحميل جميع الأركان بواسطة هيكل فولاذي يقوم بتوليد عزم يعمل على فتح الزاوية . تم تسجيل الإنفعالات لعدة مراحل تحميل مختلفة ولكل ركن تم فحصه كما وتم رسم منحيات الحمل والإزاحة .أثناء عملية الفحص تم رسم التشققات الحاصلة في الركن الخرساني وتحديد نوعية الفشل الحاصلة والتي كانت على نوعين(فشل إنحناء أو إرتكاز ).

لقد تبين بأن تحسين خواص الخرسانة يؤدي الى زيادة الكفاءة كبديل لتقليل حديد القص والتفصيل المعقدة لحديد التسليح في الاركان المعرضة لعزوم انحناء تعمل على فتح الزاوية بالاضافة الى تاثيرها على مقاومة ونوع الفشل الحاصل في الركن الخرساني.

بالإعتماد على النتائج المستحصلة من البحث الحالي تم إختيار احد النماذج باعتباره مناسب للاعمال الانشائية الخاصة للابنية المعرضة للهزات والزلازل الارضية .

**NOMENCLATURE**

$b_f$ =Width of compression face of member, (mm)

D =distance from extreme compression fiber to centroid of longitudinal tension reinforcement, (mm)

$f'_c$= cylinder compressive strength of concrete, (MPa)

$f_y$= specified yield strength of reinforcement, (MPa)

$M_{cr}$=first cracking moment, (kN.m)

$(M_{cr})_R$ =first cracking moment of reference corner, (kN.m)

$M_u$=ultimate moment at section, (kN.m)

$(M_u)_R$ =ultimate moment of reference corner, (kN.m)

## INTRODUCTION

The joint formed from two adjacent members at 90$^o$ usually refers to the "corner". The terms "opening" and "closing" the corner are used to describe the increase and decrease of this right angle [1], respectively. Concrete corners are found in wide variety of structures such as retaining walls, bridges and portal frame buildings. They are also common in the field of hydraulic structures, such as reservoirs, tanks, flumes and culverts. In general, the failure of opening corners is invariably characterized by the low tensile strength of concrete resulting in the initiation of a splitting tensile crack originating at the reentrant corner and gradually moves out along the corner diagonal towards the exterior corner [2] and [3].

## Dimensions of Tested Corners

The nominal dimensions of the tested corners are as shown in **Figure (1)**. Also, the cross section details and the inner and outer angle of corner is right angle (90 ◦). The corner pad is (70mm) in height and (70mm) in width.

## Reinforcement Details

The reinforcement detail used in this work is constant for all corners which is simple detail as shown in **Figure (1).**

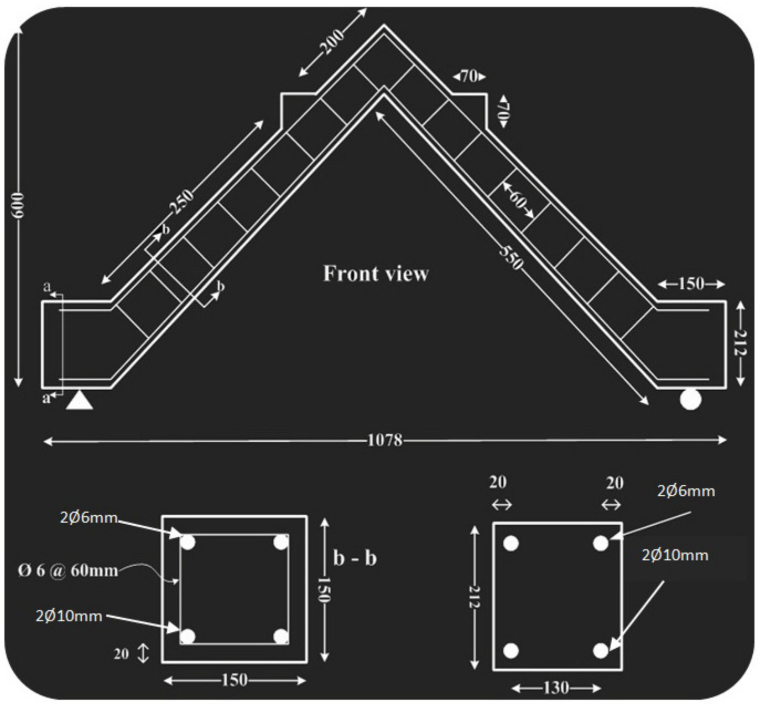


**Figure (1), Dimension of the tested corners**

## Parameters

Four parameters control the specimens which are percentages of steel fiber volume fraction Vf (0.5% and 1.5%), silica fume (5% and 10%), percentages of (fine sand/fine gravel) (70/30 % and 50/50 %), finally the presence or absence of main longitudinal reinforcement, as shown in the **Table (1).** These specimens were loaded up to failure to study the influence of these variables on the strength and behavior of MRPC knee joints in bending.

**Table (1) Properties of tested corners**

| Corners No. | G11 | G12 | G21 | G22 | G31 | G32 | G41 | G42 | G51 | G52 | G61 | G62 |
|---|---|---|---|---|---|---|---|---|---|---|---|---|
| Status | NSC* | NSC | MRPC** | MRPC | MRPC | MRPC | MRPC | MRPC | MRPC | MRPC | MRPC | MRPC |
| Tension Rebar | 2Φ10 mm | 2Φ10 mm | 2Φ10 mm | 2Φ10 mm | 2Φ10 mm | 2Φ10 mm | 2Φ10 mm | 2Φ10 mm | 2Φ10 mm | 2Φ10 mm | Nil | Nil |
| Cement content $kg/m^3$ | 400 | 400 | 900 | 900 | 900 | 900 | 900 | 900 | 900 | 900 | 900 | 900 |
| Sand 4.75 mm ($kg/m^3$) | 600 | 600 | --- | --- | --- | --- | --- | --- | --- | --- | --- | --- |
| Gravel 10 mm ($kg/m^3$) | 1200 | 1200 | --- | --- | --- | --- | --- | --- | --- | --- | --- | --- |
| Fine sand 0.6mm ($kg/m^3$)<br><br>% of Total Aggregate | --- | --- | 693<br><br>70 | 495<br><br>50 | 693<br><br>70 | 495<br><br>50 | 693<br><br>70 | 495<br><br>50 | 693<br><br>70 | 495<br><br>50 | 693<br><br>70 | 495<br><br>50 |
| Fine gravel 4,75mm ($kg/m^3$)<br><br>% of Total Aggregate | --- | --- | 297<br><br>30 | 495<br><br>50 | 297<br><br>30 | 495<br><br>50 | 297<br><br>30 | 495<br><br>50 | 297<br><br>30 | 495<br><br>50 | 297<br><br>30 | 495<br><br>50 |
| Total aggregate ($kg/m^3$) | --- | --- | 990 | 990 | 990 | 990 | 990 | 990 | 990 | 990 | 990 | 990 |
| Mix proportions (cement : sand : gravel) | 1 : 1.5 : 3 | 1 : 1.5 : 3 | 1 : 0.77 : 0.33 | 1 : 0.55 : 0.55 | 1 : 0.77 : 0.33 | 1 : 0.55 : 0.55 | 1 : 0.77 : 0.33 | 1 : 0.55 : 0.55 | 1 : 0.77 : 0.33 | 1 : 0.55 : 0.55 | 1 : 0.77 : 0.33 | 1 : 0.55 : 0.55 |
| W/C ratio | 0.45 | 0.45 | 0.25 | 0.25 | 0.25 | 0.25 | 0.25 | 0.25 | 0.25 | 0.25 | 0.25 | 0.25 |
| Steel fiber % of total volume | 0 | 0.5 | 0.5 | 0.5 | 0.5 | 0.5 | 1.5 | 1.5 | 1.5 | 1.5 | 0.5 | 0.5 |
| Silica fume % of cement | 0 | 0 | 5 | 5 | 10 | 10 | 5 | 5 | 10 | 10 | 10 | 10 |

*NSC: Normal Strength Concrete

**MRPC: Modified Reactive Powder Concrete

## Testing of Corners

All corner specimens are tested by using the universal testing machine (MFL system) under monotonic loads up to failure, as shown in the **Figure (2)**. According to the circumstances of this test, the specimen (concrete corner) is supported to be hinged at one leg and rolled in the other leg upon this apparatus, using two clamps in one side to achieve the hinged situation.

**Figure (2), Universal testing machine**

The upper and lower parts of concrete corner are modified to make the applied loads act as a coupled situation on each side, this leads to open the corner at center, as shown in **Figures (3).**

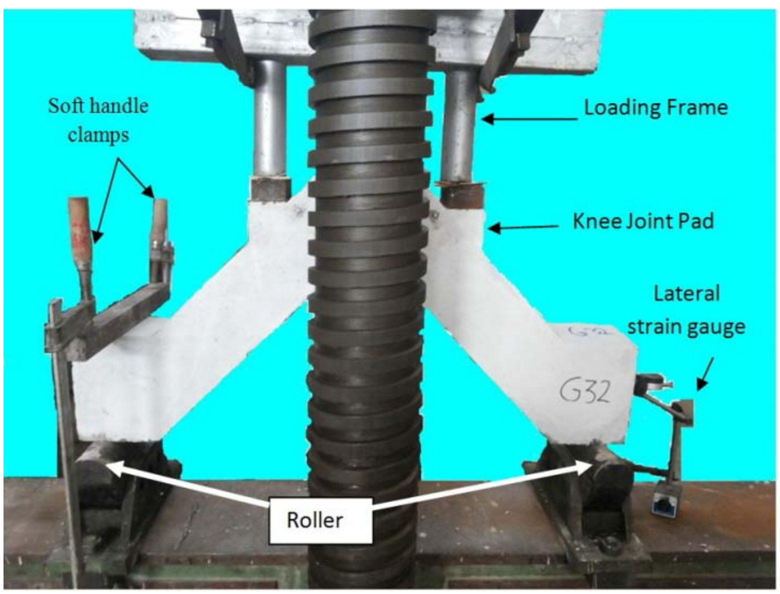


**Figure (3), corner setup**

The applied loads are concentrated by adjustment of steel frame that has two legs settled on the specimen's pad under hydraulic jack. Thin wooden patches are inserted between the concrete and points of loads to provide even surface. The loads are applied in successive increments up to failure. At the end of each load increment, observations and measurements are recorded for the corner deflection, strain gauge readings and crack development and propagation on the corner surfaces.

## Types of Cracks

In the current investigation two type of cracking are found, the first one is" Flexural Cracks" usually (in most specimens). In some corners, additional flexural cracks appear at high loads, in positions nearer to the corner region and the initial cracks appear at first. Generally, the first flexural cracks appear at small percentage of the measured ultimate loading, and continue to widen and extend until they reach the compression reinforcement. Then the cracks either cease to extend or continue at a very much reduced rate but nevertheless continue to widen or extend after that. The second type is "Diagonals Cracks", these are the cracks which appear at the corner region, either at or parallel to the diagonal of corner, as shown in **Figure (4)**. At least one diagonal crack appears in each corner. Generally, this crack starts approximately in half distance between the inner and outer angles of the specimen, and continues to widen and extends at both ends until it reaches the vicinity of the main reinforcement. Then it is ceased to extend, but continues to widen until failure.

## Cracks Pattern

**Figure (4)** shows the typical crack patterns for all the tested corners under bending moment tending to open the angle. The first cracks to appear are the two cracks which are very close to the critical sections, one in each leg. These cracks extend and widen until they reach the compression zone of the section where they either terminate or change directions. While the loading processes continue, more flexural cracks appear and extend, in the same way along both legs. Diagonal crack patterns, unlike those of the flexural cracks, are different from corner to corner according to the properties of concrete.

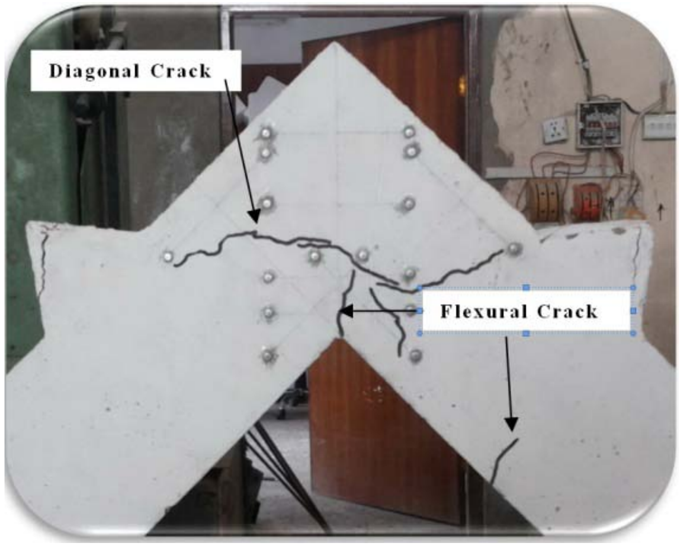


**Figure (4), Cracks Patterns and Cracks Types**

## Cracking Moments

Flexural cracks and diagonal cracks both are noticed to appear at different stages of loading. Cracking moment is that moment at which the first visible surface crack is seen by the naked eye on the surfaces of the corner. Values of the cracking moment are varying between (2.4-6.8 kN.m). And the ratio of cracking moment to the ultimate moment varies between (20.6-35.3) %. As shown in the **Table (2).** Also, a comparison is performed with first cracking moment for reference corners $(M_{cr})_R$.

**Table (2) Cracking Moments and Ultimate moments for Tested Corners**

| Corners No. | G11 | G12 | G21 | G22 | G31 | G32 | G41 | G42 | G51 | G52 |
|---|---|---|---|---|---|---|---|---|---|---|
| M crack kN.m | 2.4 | 3.1 | 5.3 | 5 | 6.2 | 6 | 5.7 | 4.9 | 6.8 | 6.3 |
| M ultimate kN.m | 6.8 | 10.2 | 22.5 | 21.7 | 25.2 | 24.7 | 25.7 | 23.8 | 29.7 | 28 |
| $\frac{\text{M crack}}{\text{M crack refernce}}$ | 1 | 1.29 | 2.2 | 2.08 | 2.58 | 2.5 | 2.37 | 2 | 2.83 | 2.6 |
| $\frac{\text{M crack}}{\text{M ultimate}}\%$ | 35.3 | 30.4 | 23.56 | 23 | 24.6 | 24.3 | 22.18 | 20.6 | 22.9 | 22.5 |

## Deflection

During the tests, the deflection readings are recorded at the inner angle of the corner, immediately after the application of the load. The load ─ deflection curves shown in **Figure (5),** for the corners tested under bending moment tend to open the angle up to failure. In this figure, the curves in general consist of three parts each; The first part, starts form zero load up to the formation of the first flexural cracks, is of relatively steeper slope which in turn means that the corners at this stage are of relatively higher flexural rigidity. The second part of the load deflection curve extends from the point of the first yielding to the point at which yielding of all reinforcement takes place at any of the two critical sections or both. The third and final part of the load deflection curve extends from the point of yielding at the critical section to failure of corner. This part is relatively linear and the corners at this stage have little rigidity in flexure.

The deflection at ultimate load for all tested corners is shown in **Table (3)**; this table shows the increase in total deflection for all corners when compared with reference corner deflection. The increase in total deflection is mainly caused by the lack of reinforcement in the region of the corner [4].

**Table (3), Deflection values at ultimate load for all tested corners**

| **Corners No.** | **G11** | **G12** | **G21** | **G22** | **G31** | **G32** | **G41** | **G42** | **G51** | **G52** |
|---|---|---|---|---|---|---|---|---|---|---|
| **Δ* (mm)** | 3.4 | 4.5 | 12.5 | 13 | 12 | 12.4 | 19.7 | 20.5 | 19.1 | 19.3 |
| **Δ/ΔR % **** | 100 | 132 | 367 | 382 | 353 | 364 | 579 | 603 | 561 | 567 |

*Δ= deflection value at ultimate load for corners specimen.

**ΔR= deflection value at ultimate load for reference corner G11=3.4 mm.

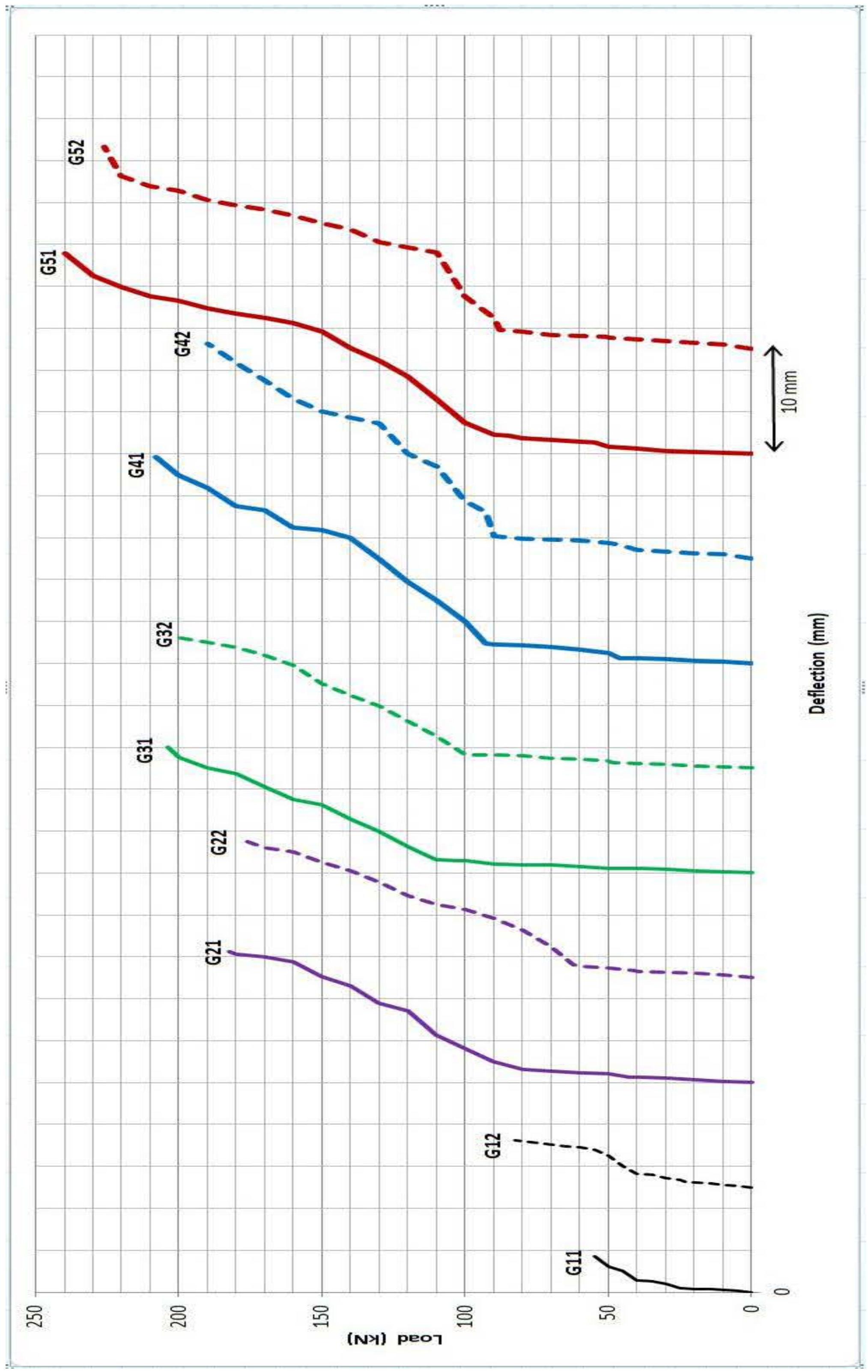


**Figure (5), Load Deflection curve for all tested corners**

## Concrete Strain

**Figure (6),** represents the concrete strain versus depth at load 20 kN for all steel reinforced tested corners where the strain for ten specimens has maximum value at the inner corner and it is tensile in nature as a result for that, the inner corner is subjected to high biaxial state of tensile stresses resulting in cracking at the inner corner along the diagonal.

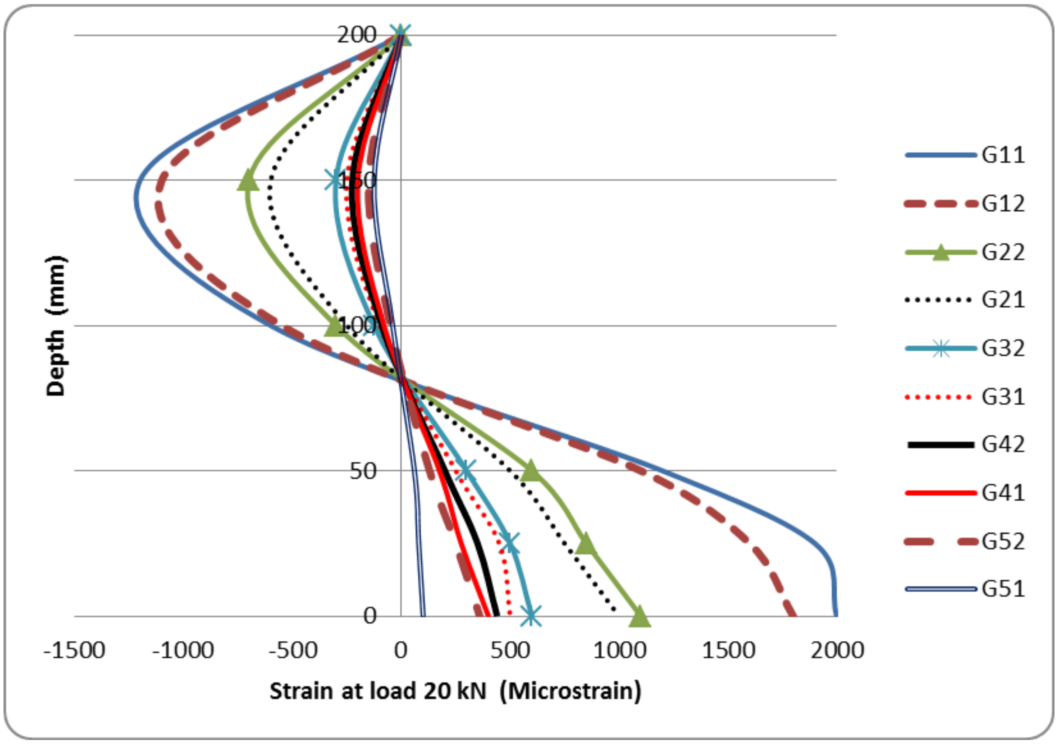


**Figure (6), concrete strain curve versus depth at load 20 kN for all knee joints**

Also**, figure (7)** represents the correlation between the strains at different stages of loading against the depth of corner block G51. In some corners, tensile stress value is higher than the tensile strength of concrete, this may cause cracking and pushing out of the concrete.

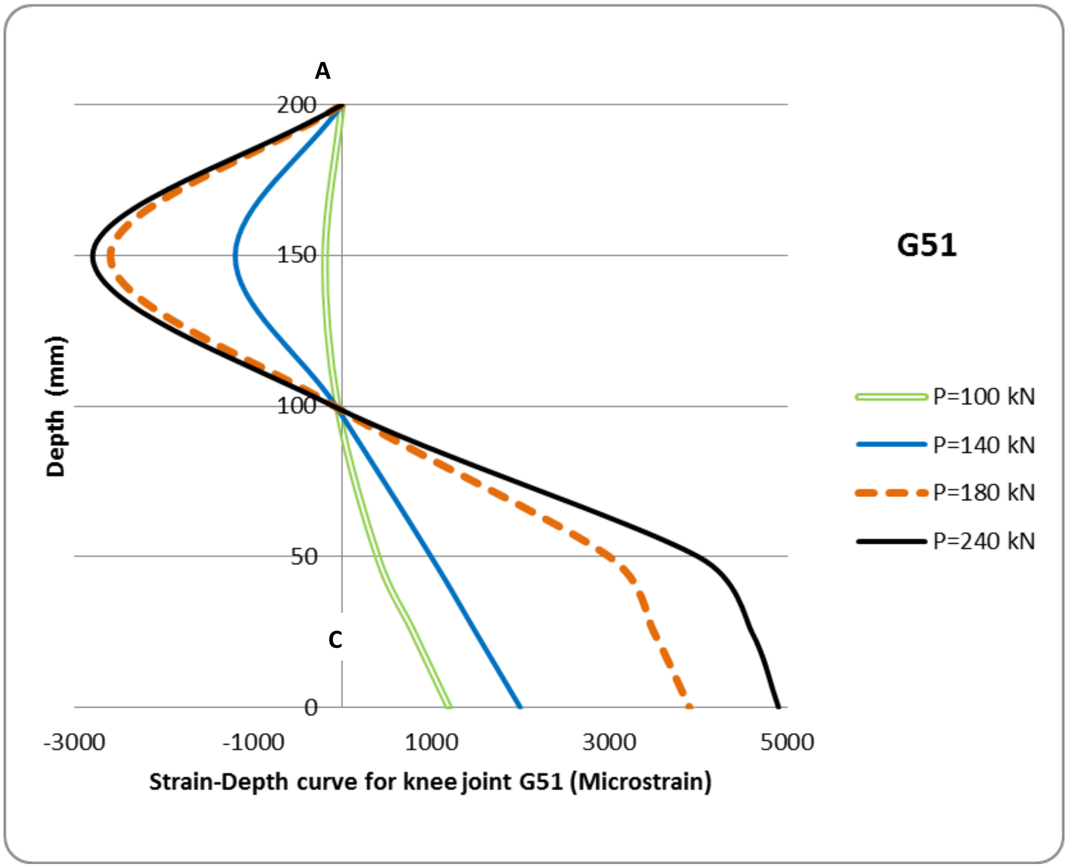


**Figure (7), the correlation between the strains at a different stage of loading against the depth of corner block G51**

## Mode of Failure

The corners subjected to bending moment tend to open the angle generally have two types mode of failure. The first type is the flexural failure. This type of failure usually takes place in the legs of the corner. However, flexural failure may also take place in corners containing diagonal corner cracks, especially when the reinforcement is not heavy. In the present work, all corners failed due to flexural cracks except G11 and G51. The second type of failure is the bearing failure. This type of failure usually takes place due to diagonal crack of corners with heavy reinforcement. The failure occurred at a moment less than that predicted by the ultimate load flexure method, as shown in corner G11. **Table (4)** shows the mode of failure for all corners.

**Table (4), concrete knee joints mode of failure**

| Corners No. | G11 | G12 | G21 | G22 | G31 | G32 | G41 | G42 | G51 | G52 | G61 | G62 |
|---|---|---|---|---|---|---|---|---|---|---|---|---|
| Mode of failure at corner block | Bearing | Flexural | Flexural | Flexural | Flexural | Flexural | Flexural | Flexural | No failure at corner block | Flexural | Flexural | Flexural |

## Ultimate Strength of Corners

Ultimate moment is the maximum moment which could be carried out by the tested corners. It is evident that the theoretical moment results of the steel reinforced NSC and MRPC specimens varies between (9.82 and 10.7) kN.m; also the experimentally results of the ultimate moment varies between (6.8 and 29.7) kN.m. The experimental moment results for all steel reinforced NSC and MRPC knee joints are greater than theoretical (predicted) moment except NSC knee joint G11 as shown in the **Figure (8).** This means that G11 fail before reach the theoretical design strength. The ultimate moment increased by the presence and/or increment of steel fiber content when the other parameters fixed. This is due to the fact that steel fibers act as micro-reinforcement and crack arrester similar to flexural steel reinforced in conventional reinforced concrete. After cracking, steel fibers seem to be capable to bear further tensile loads until they are pulled out. For steel reinforced MRPC corners the addition of silica fume increases the ultimate moment when the other parameters fixed. That could be attributed to the matrix densification, which means: The presence of silica fume in the concrete mixes cause a reduction in the volume of the pores. It basically acts as filler due to its fineness. Hence mechanical properties are improved because of the enhancement of the bond strength. For MRPC, the ultimate moment increased by the increase of fine aggregate proportions when other parameters fixed, which means the increase of fine sand percentage with respect to fine gravel, due to the bond strength between paste and steel reinforced, bond between past and steel fiber and the bond between the paste and the aggregate.

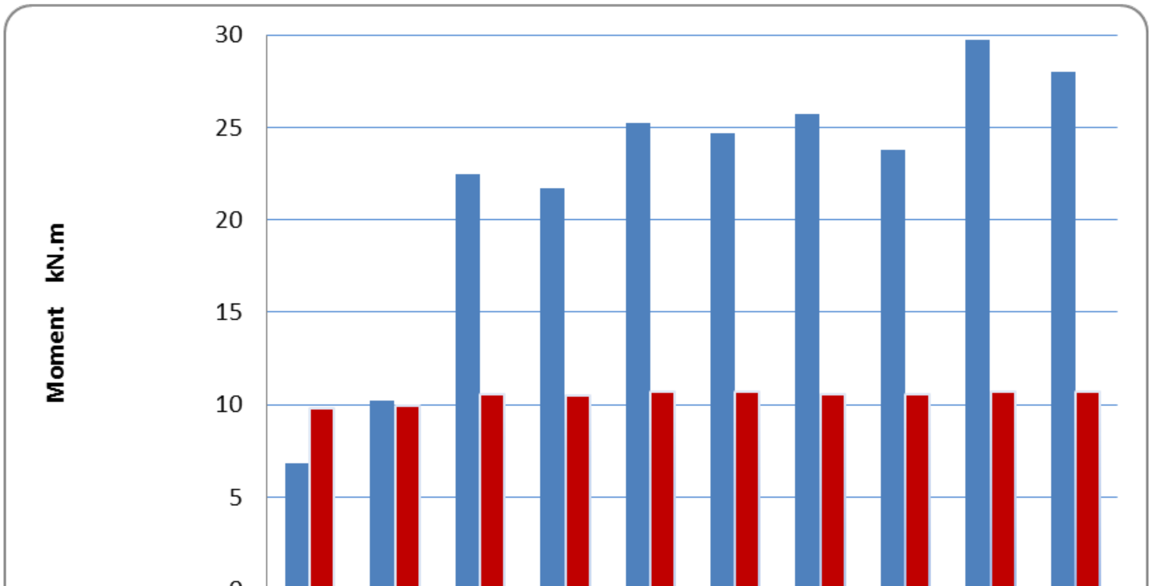


| | G11 | G12 | G21 | G22 | G31 | G32 | G41 | G42 | G51 | G52 |
|---|---|---|---|---|---|---|---|---|---|---|
| M ultimate test kN.m | 6.8 | 10.2 | 22.5 | 21.7 | 25.2 | 24.7 | 25.7 | 23.8 | 29.7 | 28 |
| M cal. kN.m | 9.82 | 9.9 | 10.55 | 10.51 | 10.68 | 10.66 | 10.58 | 10.54 | 10.7 | 10.67 |

**Figure (8), Theoretical and experimental results of moment**

## Corners Efficiency

The efficiency of a corner is defined as a ratio of the strength of the corner from a test to the theoretical strength of the corner [1]. The results show that the efficiency of corners vary between (G11 and G51) by (69 to 277)% respectively, where all the corners are efficient except the NSC reference corner G11 was deficient and would be unsafe in design, as shown in the **Figure (9)**. The normal strength concrete could not bear the applied moment; therefore enhance the concrete properties using steel fiber with MRPC will improve the strength. In this case there is no need for shear steel or steel reinforcement with complicated details in the corner block. The randomly oriented steel fibers and the ability of steel fibers to arrest cracking widened process cause an increase in the tensile load capacity beyond the first cracking, and that lead to increase the efficiency. For steel reinforced MRPC knee joint specimens, the addition of silica fume increases the efficiency, when the other parameters fixed. The efficiency increased by the increase the percentage of fine aggregate ingredient proportions for the corners.

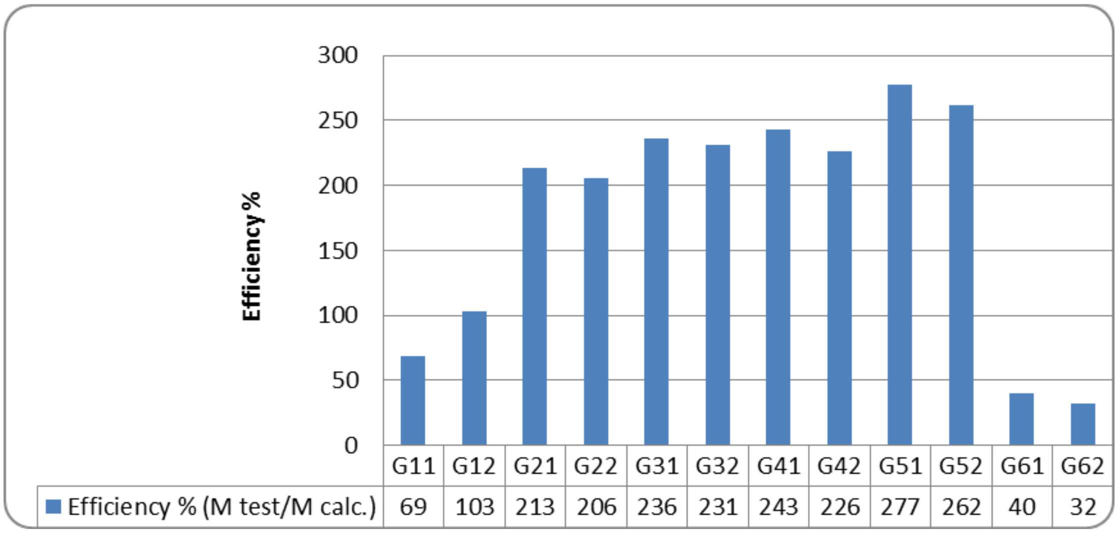


**Figure (9) Efficiency of all corners**

## Ductility

Ductility is described as the ability of a structural element to sustain inelastic deformation without significant loss in resistance [5]. It is necessary for many reasons including safety, possible redistribution of load or moment, and design of structures subjected to seismic loading[6]. The ductility is an important property for safe structural design in the seismic countries. Also, the ductility is an important characteristic of any structural element. In this work the ductility investigated by two methods, theoretically by applying equations and experimentally by calculates the area beneath the load-deflection curve. Theoretical Ductility can be defined as the ratio of the curvature at ultimate moment to the curvature at yield, [6] and [7].

$$\text{Ductility} = \mu = \frac{\varphi_u}{\varphi_y} = \frac{\varepsilon_u}{fy/Es} * \frac{d(1-k)}{\frac{a}{\beta_1}} \qquad \ldots\ldots [6] \ldots (\text{Eq.}-1)$$

$$\text{Ultimate condition} = \varphi_u = \frac{\varepsilon_{c.u}}{c} = \frac{\varepsilon_{c.u} * \beta_1}{a} \qquad \ldots\ldots [6] \ldots\ldots (\text{Eq.}-2)$$

Yield condition: $\varphi_y = \frac{fy}{Es} * \frac{1}{d*(1-k)}$ .....[6]....(Eq.-3)

$$k = \left[(\rho + \rho')^2 * n^2 + 2 * \left\{\rho + \frac{\rho' * d'}{d}\right\} * n\right]^{\frac{1}{2}} \quad .....[6]....(Eq.-4)$$

$$a = \frac{As * fy - As' * fy'}{0.85 * f'c * b} \quad .....[6]....(Eq.-5)$$

$$n = \frac{\text{Modulus of elasticity for steel } (E_s)}{\text{Modulus of elasticity for concrete } (E_c)} \quad .....[6]....(Eq.-6)$$

$$\rho = \frac{A_s}{b * d} \quad .....[6]....(Eq.-7)$$

$$\rho' = \frac{A_s{}'}{b * d'} \quad .....[6]....(Eq.-8)$$

$$\varepsilon_{c.u} = 0.003 \quad .....[6]....(Eq.-9)$$

$$\beta_1 = 0.85 \quad .....[6]....(Eq.-10)$$

$A_s$ = Area of tension steel reinforcement ($mm^2$)

$A_s'$ = Area of compression steel reinforcement ($mm^2$)

d = Distance from center of tension rebar to extreme compression (mm)

d' = Distance from center of compression rebar to extreme compression (mm)

fy = yeild tesile strength of steel (Mpa)

$f'c = compressive\ strength\ \ (Mpa)$

The theoretical ductility value varies between (G11 and G51) by ductility value (3.11 and 15.24) respectively, and the experimental ductility index value varies between (G11 and G42) by the ductility value (1.29 and 32.92) respectively. It is obvious that all the experimental ductility values results of the steel reinforced MRPC knee joints are greater than the values of theoretical ductility except G31. Also, the values of the theoretical ductility not proportioned with the values of the experimental ductility index in the same ascending sort, as shown in the **Figure (10).**

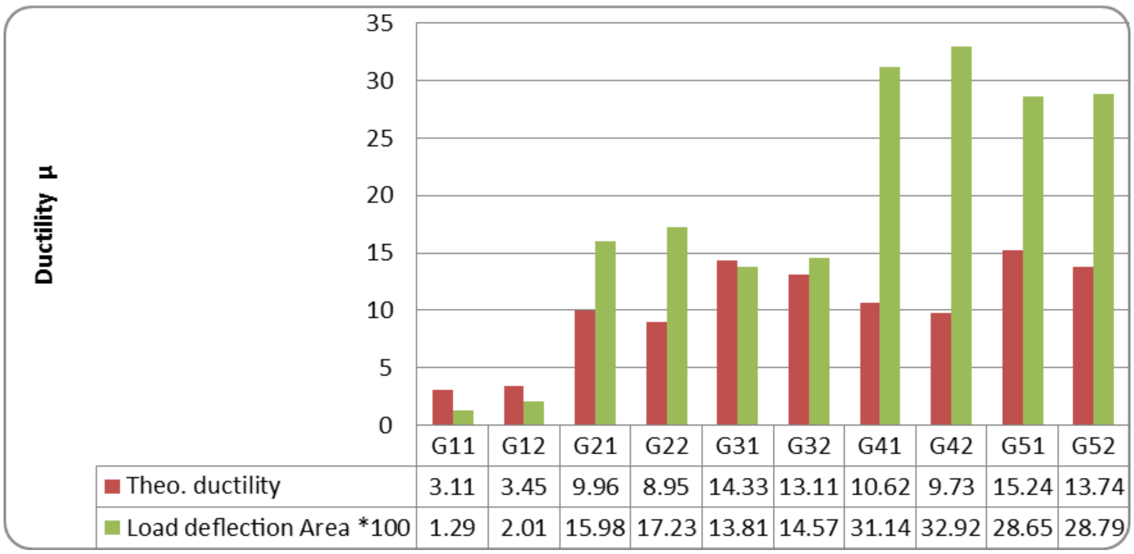


| | G11 | G12 | G21 | G22 | G31 | G32 | G41 | G42 | G51 | G52 |
|---|---|---|---|---|---|---|---|---|---|---|
| Theo. ductility | 3.11 | 3.45 | 9.96 | 8.95 | 14.33 | 13.11 | 10.62 | 9.73 | 15.24 | 13.74 |
| Load deflection Area *100 | 1.29 | 2.01 | 15.98 | 17.23 | 13.81 | 14.57 | 31.14 | 32.92 | 28.65 | 28.79 |

**Figure (10), comparison between theoretical and experimental Ductility**

## CONCLUSIONS

The following conclusions are drawn only from the twelve corners studied in this investigation:

1- The knee joint G51 present the goal of this study because no cracks appear at corner block. The efficiency of 277% due to enhancing the properties of concrete therefore no need for much reinforcement at corner block. Also, G51 was the most influential corner which reveals the maximum values of constituent properties and maximum values of structural properties except the ductility. In contrast, the second descending most influential corner sorted after specimen G51 was the knee joint G31which represents reasonable efficiency 236%. The point of interest is, increasing the steel fiber in MRPC with high content of silica fume will not improve the properties as much as expected.

2- The corner G42 gained the maximum value of experimental ductility index (32.92). Therefore, G42 considered the sufficient specimen for seismic and earthquake regions than the other knee joints. In contrast, the corner G31 possessed the minimum ductility index (13.81) than the other corners.

3- The use of steel fibers does not generally lead to an increase in compressive strength. But the results showed that for all corners the compressive strength is only slightly increase by the addition of steel fibers.

4- Increase steel fiber content for NSC and MRPC corners will increase the cracking moment, ultimate moment, efficiency and experimental ductility. In contrast increase the steel fiber will decrease the strain.

5- The increase of silica fume content in MRPC corners will increase the cracking moment, ultimate moment and efficiency. In contrast, increase silica fume will decrease the strain, experimental ductility and the deflection at the ultimate load.

6- The increase the fine aggregate proportions (fine sand/fine gravel) for the MRPC corners will increase the cracking moment, ultimate moment and efficiency, while this will decrease the strain, experimental ductility and the deflection at the ultimate load.

7- Silica fume and steel fiber were the most effected parameters on efficiency and ultimate moment.

8- Steel fiber was the most effected parameter on the experimental ductility and deflection at the ultimate load.

9- The structural properties of MRPC influenced by steel fiber and silica fume more than the percentage of (fine sand/fine gravel).

## REFERENCE


1- Mayfield B., Kong F. K. and Bennison A., "Strength and stiffness of lightweight concrete corners", ACI Journal, Vol.69, No.38, July 1972, pp. 420-427.

2- Nilsson, I.H.E., "Reinforced Concrete Corners and Joints Subjected to Bending Moment", National Swedish Building Research, Sweden, 1973, P.P. 244.

3- Nilsson I.H.E. and Losberg A.,"Reinforced concrete corners and joints subjected to bending moment" Proceeding ASCE, Vol.102, No.6, 1976, pp.1229-1254.

4- Nilson, A.H., Darwin D. and Dolan CH. W. " Design of Concrete Structures" Thirteenth Edition, The MacGraw-Hill Edition, 2004, 366p.

5- Naaman A.E., Harajli M.H., and Wight J.K. (1986). Analysis of ductility in partially prestressed concrete flexural members. PCI Journal, 31:3, 64-87.

6- Park R. and Paulay T., "Reinforced Concrete Structures", John Wiley and Sons, 1975, pp.195-761.

7- Oral Buyukozturk, “Mechanics and design of concrete structures”, Massachusetts institute of technology, spring 2004,outline 6 ductility and deflections, pp. 1-9.